The histone H1 C-terminal domain binds to the apoptotic nuclease, DNA Fragmentation Factor (DFF40/CAD) and stimulates DNA cleavage

ARTICLE *in* BIOCHEMISTRY · JUNE 2005

Impact Factor: 3.02 · DOI: 10.1021/bi050100n · Source: PubMed

6 AUTHORS, INCLUDING:

Piotr Widlak
Maria Sklodowska Curie Memorial Cancer Ce…
119 PUBLICATIONS **2,011** CITATIONS
SEE PROFILE

Missag H Parseghian
Rubicon Biotechnology
25 PUBLICATIONS **713** CITATIONS
SEE PROFILE

Jeffrey C Hansen
Colorado State University
118 PUBLICATIONS **6,907** CITATIONS
SEE PROFILE

The Histone H1 C-Terminal Domain Binds to the Apoptotic Nuclease, DNA Fragmentation Factor (DFF40/CAD) and Stimulates DNA Cleavage†

Piotr Widlak,‡,§ Magdalena Kalinowska,§ Missag H. Parseghian,|| Xu Lu,⊥ Jeffrey C. Hansen,⊥ and William T. Garrard*,‡

Department of Molecular Biology, University of Texas Southwestern Medical Center, Dallas, Texas 75235, Department of Experimental and Clinical Radiobiology, Maria Sklodowska-Curie Cancer Center and Institute of Oncology, 44-100 Gliwice, Poland, Peregrine Pharmaceuticals, Inc., 14272 Franklin Avenue, Suite 100, Tustin, California 92780, and Department of Biochemistry and Molecular Biology, Colorado State University, Fort Collins, Colorado 80523-1870

Received January 18, 2005; Revised Manuscript Received April 5, 2005

ABSTRACT: The apoptotic nuclease, DNA fragmentation factor (DFF40/CAD), is primarily responsible for internucleosomal DNA cleavage during the terminal stages of programmed cell death. Previously, we demonstrated that histone H1 greatly stimulates naked DNA cleavage by this nuclease. Here, we investigate the mechanism of this stimulation with native and recombinant mouse and human histone H1 species. Using a series of truncation mutants of recombinant histone H1-0, we demonstrate that the H1 C-terminal domain (CTD) is responsible for activation of DFF40/CAD. We show further that the intact histone H1-0 CTD and certain synthetic CTD fragments bind to DFF40/CAD and confer upon it an increased ability to bind to DNA. Interestingly, we find that each of the six somatic cell histone H1 isoforms, whose CTDs differ significantly in primary sequence but not amino acid composition, equally activate DFF40/CAD. We conclude that the interactions identified here between the histone H1 CTD and DFF40/CAD target and activate linker DNA cleavage during the terminal stages of apoptosis.

The repeating subunit of eukaryotic chromatin is the nucleosome, which is composed of 146 bp of DNA wrapped around an octamer of the four core histones (*1*). This beads-on-a-string configuration organizes genomes in an ideal format to be folded or coiled into a variety of higher-order structures, which can reach compaction levels approaching 10 000-fold (*2*). The linker histone, H1, is largely responsible for the stabilization of such higher-order chromatin structures (*2*, *3*).

The histone H1 molecule consists of three domains: a short, basic N-terminal domain (NTD),[1] a highly conserved central globular domain (GD), and a basic C-terminal domain (CTD) (*4*). Although it was initially thought that the central GD was responsible for the stabilized binding of histone H1 to the nucleosome near the points of entry and exit of the wrapped DNA turns (*5*), recent in vitro and in vivo experiments demonstrate that the ability of histone H1 to bind to chromatin and to mediate folding and condensation are largely conferred by the basic CTD of the protein (*6*, *7*). This domain is unstructured in the absence of DNA, but believed to become structured upon DNA binding (*6*). Histone H1 species consist of a family of six different protein isotypes in somatic cells of the mouse (*4*). Gene knockout experiments reveal that these isotypes serve semiredundant functions, as embryonic lethality requires triple-H1-nulls (*8*).

It is interesting to reflect from an evolutionary point of view that nucleosome structure not only fulfills crucial regulatory and packaging roles in living cells, but it also prepares dying cells for the efficient clearance of DNA by phagocytosis during programmed cell death or apoptosis. Indeed, one of the hallmarks of the terminal stages of apoptosis is the processing of genomic DNA by apoptotic nucleases into "bite-size" mononucleosome pieces. This processing has functional significance because cell-autonomous DNA breakdown of tumor or virally infected cells prepares the resulting apoptotic corpses for engulfment by phagocytes and, as such, eliminates the transforming potential of any hazardous oncogenes (*9*). In addition, a predisposition to autoimmune disease is seen in patients or an animal model with defective apoptotic DNA processing, a disease known to be associated with the appearance of anti-DNA and anti-nucleosomal antibodies (*10*, *11*). Here, we study one of the major apoptotic nucleases, termed DNA

† This work was supported in part by Grant 3P05A10424 from the Committee for Scientific Research KBN (to P.W.), Grants GMRO1-59809 and GMRO1-29935 from the National Institutes of Health and Grant I-0823 from the Robert A. Welch Foundation (to W.T.G.), and NIH Grant 45916 (to J.C.H).

* Address correspondence and reprint requests to Dr. William T. Garrard, Department of Molecular Biology, University of Texas Southwestern Medical Center, 5323 Harry Hines Blvd., Dallas, TX 75390-9148. Phone: 214-648-1924. Fax: 214-648-1915. E-mail: william.garrard@utsouthwestern.edu.

‡ University of Texas Southwestern Medical Center.

§ Maria Sklodowska-Curie Cancer Center and Institute of Oncology.

|| Peregrine Pharmaceuticals, Inc.

⊥ Colorado State University.

[1] Abbreviations: Ac-DEVD-Cho, acetyl-Asp-Glu-Val-Asp-aldehyde; DFF, *D*NA *f*ragmentation *f*actor; CAD, *c*aspase *a*ctivated *d*eoxyribonuclease (also termed DFF40); CIDEs, *c*ell death-*i*nducing *D*FF45-like *e*ffectors; CPAN, *cas*pase *a*ctivated *n*uclease (also termed DFF40 and CAD); CTD, C-terminal domain; DFF45, 45-kD subunit of DFF; DFF40, 40-kD subunit of DFF; GD, globular domain; ICAD-L, *i*nhibitor of *CAD*, *l*ong form (also termed DFF45); MNase, micrococcal nuclease; NTD, N-terminal domain; SDS−PAGE, sodium dodecyl sulfate−polyacrylamide gel electrophoresis.

10.1021/bi050100n CCC: $30.25
Published on Web 05/07/2005

fragmentation factor (DFF40/CAD/CPAN) (for review, see ref *12*), whose naked DNA cleavage is greatly stimulated by histone H1 (*13*−*15*).

Recently, a specific histone H1 isotype was demonstrated to be a messenger from the nucleus to the cytoplasm, signaling DNA damage and triggering apoptosis (*16*). Upon DNA damage, histone H1.2 was shown to leak to the cytoplasm, trigger the release of cytochrome c from mitochondria, and initiate apoptosis (*16*) (we designate this histone species as H1-1 in the nomenclature used here, ref *17*). This signaling could be reconstituted with recombinant H1-1 in vitro, and a knockout mouse lacking functional H1-1 genes was resistant to apoptotic stimuli (*16*).

In the present study, we have characterized the effects of the six somatic isotypes to test the hypothesis that H1-1 might be a preferential activator of DFF40/CAD. We also have used recombinant technology to dissect the histone H1 domains responsible for DFF40/CAD activation. Our results demonstrate that the H1 CTD, as well as select CTD fragments, bind to DFF40/CAD and endow it with the increased ability to bind to DNA. All somatic isotypes were equally capable of stimulating nuclease activity in vitro, suggesting that CTD amino acid composition is more important than primary sequence.

EXPERIMENTAL PROCEDURES

Expression, Purification, and Activity Assay of Recombinant Forms of DFF. Human hexa-His-tagged DFF40 was coexpressed in a polycistronic vector with human DFF45 and purified as described previously (*14*). Mouse GST-tagged CAD was coexpressed with human DFF45 using a two-vector system described previously (*18*). The GST-fusion protein was purified on GSH-Sepharose and the GST tag removed by thrombin cleavage. One milligram of GST-CAD was incubated with 50 units of thrombin for 2 h at room temperature, and then the resulting CAD/DFF45 heterodimer was purified by Q-Sepharose chromatography using a linear 0.1−0.35 M NaCl gradient. Hamster recombinant caspase-3 was expressed in *Escherichia coli* and purified as described previously (*14*). DFF heterodimer (50 ng; 0.5 pmol) was activated by incubation with caspase-3 (0.1 pmol) at room temperature in buffer consisting of 10 mM KCl, 1 mM EGTA, 1 mM DTT, and 20 mM Tris-HCl, pH 7.5. After 20 min of incubation, caspase-3 was inhibited with 10 μM Ac-DEVD-Cho. Nuclease activity was assayed as described previously (*15*). As substrate, we used pWLTR11 plasmid DNA, which is a 4.2 kb sequence containing a 1.4 kb fragment of the HIV-1 genome LTR inserted into pNEB193 (*19*). However, the effects of H1 upon DFF40 cleavage were the same irrespective of what type of plasmid DNA was used as a substrate. Briefly, 1 μg of pWLTR11plasmid DNA, $MgCl_2$ (4 mM final), and NaCl (100 mM final) was added to activated DFF (final volume 20 μL) and incubated for 30 min at 33 °C, and then the reaction was stopped by adding EDTA, SDS, and Proteinase K. In some experiments, fresh DFF45 (20-fold molar excess as compared to the starting DFF heterodimer concentration) and/or histone H1 (usually 200 ng; ~10 pmol) was added to the activated DFF mixture (with 5 min incubation on ice) before adding DNA substrate. The majority of experiments were repeated with both human DFF40 and mouse CAD without any discrepancies in the results obtained.

Purification of Histone H1 Subtypes. Human and murine linker histones were isolated from human placenta and mouse liver, respectively, using an acid extraction procedure as described elsewhere (*20*). Once the H1 histones were isolated, the subtypes were purified by a modified form of cation-exchange-hydrophilic-interaction chromatography (CX-HILIC; ref *21*). Details of the method and its modifications will be described elsewhere (Parseghian, manuscript in preparation). Briefly, human H1 subtypes were fractionated on a weak cation exchange column, known as PolyCAT A (PolyLC, Columbia, MD), using a shallow sodium perchlorate ($NaClO_4$) gradient of 0.25 mM/min from 340 to 350 mM at a flow rate of 0.6 mL/min. Similarly, mouse H1 subtypes were purified using a $NaClO_4$ gradient of 0.25 mM/min from 350 to 360 mM at a flow rate of 0.6 mL/min. The running buffers, Buffer A [50% acetonitrile and 50 mM phosphoric acid, pH 6.5] and Buffer B [50% acetonitrile, 50 mM phosphoric acid, and 800 mM $NaClO_4$, pH 4.0] were degassed with helium prior to use on a Beckman System Gold HPLC (Beckman Coulter, Fullerton, CA). Fractions were collected and dialyzed against 10 mM HCl to remove residual perchlorate prior to lyophilization. When total histone H1 species were used, they were purified from HeLa cell chromatin using hydroxyapatite as described elsewhere (*15*).

Expression and Purification of H1-0 Proteins and Peptides. Wild-type H1-0 and various domain mutants were constructed using the same standard procedures (*22*) as in the previous work (*6*). All H1-0 proteins were expressed and purified as described (*6*), except that a HiTrap SP HP column was used in the place of a CM-Sephadex C-25 column for H1-0 CTD 97−169 and 97−145 species. Peptides 121−145, 122−169, and 146−193 were synthesized on a Perseptive Biosystems Pioneer automated peptide synthesizer (Applied Biosystems, Foster City, CA) using optimized Fmoc chemistry (*23*). The crude peptides were then purified by reversed-phase HPLC on a Waters liquid chromatography system using a Vydac C_4 semipreparative column (250 mm × 10 mm). The identity of the purified peptides was confirmed by electrospray mass spectrometry on a VG Quattro II triple quadrupole instrument.

Native Pore-Exclusion Limit Electrophoresis. Native pore-exclusion limit electrophoresis was performed as described elsewhere (*24*). Briefly, purified proteins (at amounts described in figure legends) were incubated for 15 min on ice in buffer consisting of 10 mM KCl, 100 mM NaCl, 1 mM EDTA, 1 mM DTT, and 20 mM Tris-HCl, pH 7.5, and then separated on linear 4%−24% gradient polyacrylamide gels in 0.1 M Tris-borate, pH 9.5, 1 mM β-mercaptoethanol for 16 h at 300 V, ~10 mA, at 4 °C (gels were calibrated by coelectrophoresis of different molecular size markers). Gels were soaked in 0.5% SDS, 25 mM Tris-Cl, and 250 mM glycine, pH 8.5, and then proteins were electrophorectically transferred onto nitrocellulose membranes and immunodetected as described below.

Western Blot Analyses. Proteins were separated on SDS−14% polyacrylamide gels and electrophoretically transferred onto nitrocellulose membranes (Schleicher & Schuell). Membrane-immobilized proteins were probed with the following commercial antibodies: rabbit anti-human DFF40 polyclonal antibodies (Axxora), rabbit anti-human DFF45 N-terminus polyclonal antibodies (Pharmingen), rabbit anti-

mouse CAD antibodies (Santa Cruz), and mouse anti-histone H1 monoclonal antibody (Santa Cruz). The antigen−antibody complexes were visualized using enhanced chemiluminescence (ECL) Western blotting detection reagents (Amersham Pharmacia Biotech).

Binding to DNA Cellulose. Inactive DFF heterodimer (1 μg) or an equivalent amount of caspase-activated DFF was incubated for 15 min on ice with histone H1 (5 μg of full-length protein and equimolar amounts of truncated proteins) in buffer consisting of 10 mM KCl, 100 mM NaCl, 1 mM EDTA, 1 mM DTT, and 20 mM Tris-HCl, pH 7.5. The mixture of the proteins was then incubated with a suspension of DNA cellulose (at an amount equivalent to 10 μg of DNA) for 30 min at 4 °C in a final volume of 500 μL of the same buffer supplemented with 0.01% Triton X-100. Cellulose beads were then washed twice with 1 mL of binding buffer. Bound proteins were eluted with 2% SDS, separated on PAGE−SDS gels, and Western-blot-detected.

RESULTS

Previous studies have shown that DFF40/CAD apoptotic nuclease is inactive in normal cells because it is bound to an inhibitor subunit, DFF45/ICAD, in a heterodimer complex (*13*, *24*−*26*). Upon exposure of cells to apoptotic stimuli, the caspase-3 protease becomes activated and cleaves the DFF45/ICAD inhibitor subunit, resulting in formation of enzymatically active DFF40/CAD homo-oligomer (*14*, *24*, *28*). We have previously shown that the abundant chromosomal protein, histone H1, greatly stimulates DFF40/CAD cleavage of both naked DNA and nucleosomal substrates in vitro (*13*−*15*). H1-dependent activation of DFF40/CAD leads to increases in the K_{cat} and decreases the K_m for naked DNA (*14*). Addition of H1 either during or after caspase-3 treatment of DFF causes the same stimulatory effect on DNA cleavage (P.W and W.T.G., unpublished), indicating that histone H1 affects DFF40/CAD enzyme activity but not caspase-3-dependent activation of the nuclease. Together, these results suggest an important role for H1 in downstream genome fragmentation during apopotosis through stimulation of DFF40/CAD activity. In the present study, we explore the molecular basis of how H1 binds to and activates DFF40/CAD in vitro. Although the in vivo substrate for DFF40/CAD is chromatin, the enzyme exclusively attacks the DNA linker between nucleosomes and does not cut nucleosome core DNA whatsoever (*15*). Hence, to directly assess the role of histone H1 on the activation process without introducing potential complicating interactions with the core histones, we chose to employ a naked DNA substrate for these studies.

Specificity of DFF40/CAD Activation by H1. Initially, several experiments were performed to examine the specificity of H1-dependent activation of DFF40/CAD in vitro. At stoichiometries equal to one histone H1 molecule per every 100−400 bp of DNA substrate, H1 maximally stimulated DNA cleavage by DFF40/CAD (Figure 1A, lanes 4 and 5). These are physiologically relevant conditions equivalent to one histone H1 per ~1−2 nucleosomes. In contrast, neither BSA nor poly-L-lysine stimulated DFF40/CAD activity (Figure 1A, lanes 1−3, 10−12). However, very minor stimulation of nuclease activity was observed with protamine (an arginine-rich protein closely related to histone H1), with poly-L-arginine, and with spermidine (a nonpeptide polycation) (Figure 1A, lanes 7−9, 13−15, 16−18). In terms of nuclease specificity, histone H1 did not activate DNase I or micrococcal nuclease (MNase) (Figure 1B). Taken together, these data demonstrate that the potent maximal activation of DFF40/CAD by histone H1 observed at physiologically relevant linker histone/DNA stoichiometries is specific for H1 and that marginal activation of DFF40/CAD can be induced by only certain specific proteins/biopolymers.

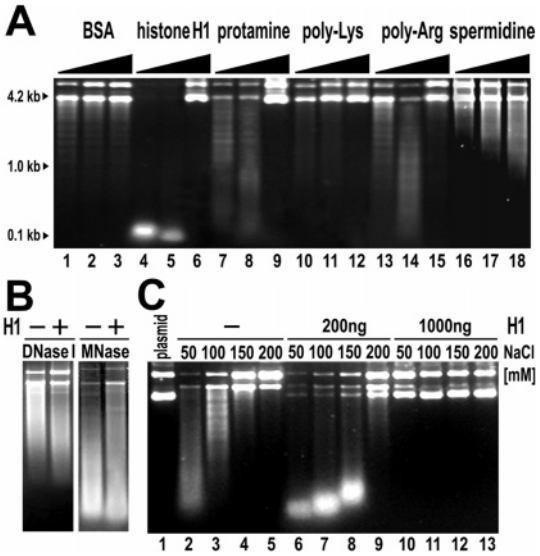

FIGURE 1: Histone H1 specifically stimulates DNA cleavage by caspase-activated DFF. (A) Plasmid DNA cleavage by caspase-activated DFF40/CAD in the presence of 100-, 250-, and 1000-ng of BSA, histone H1 (total H1 from HeLa cells), protamine (from salmon sperm), poly-L-lysine (30−70 kD), poly-L-arginine (20−70 kD), and spermidine. The DNA "band" at 0.1 kb (e.g., lane 4) actually represents fragments ranging in size between 20- and 100-bp (*15*). (B) Plasmid DNA cleavage by DNase I and micrococcal nuclease (MNase) in the presence of 200 ng of histone H1. (C) Plasmid DNA cleavage by DFF40/CAD in the presence of the indicated amounts of histone H1 with reactions carried out at 50-, 100-, 150-, and 200-mM NaCl. Reaction mixtures contained 1 μg of plasmid DNA and 0.5 pmol of DFF40/CAD, 0.001 unit of DNase I, or 0.01 unit of MNase.

Histone H1 also had a pronounced effect on the salt-dependence of DFF40/CAD activity. In the absence of H1, DFF40/CAD activity was strong (but not maximal) in 50 mM NaCl, partially inhibited in 100 mM, and completely inhibited in 150 mM (Figure 1C). In marked contrast, in the presence of H1, the activity of DFF40/CAD was maximal in 50 and 100 mM NaCl and remained robust in 150 mM NaCl at a level 2- to 3-fold lower than the maximal activity. These results demonstrate that histone H1 is able to strongly activate DFF40/CAD at higher salt concentrations where the enzyme alone is inactive.

At higher H1/DNA stoichiometries (e.g., one H1 per 20−50 bp DNA), histone H1 failed to activate DFF40/CAD (Figure 1A, lane 6; Figure 1C, lanes 10−13). No stimulatory effects of protamine and polyarginine were seen at these concentrations as well (Figure 1A, lanes 9, 15). H1, protamine, and polyarginine all can bind to DNA with modest affinities (*29*). Hence, at high stoichiometries, we believe these macromolecules are binding to the DNA substrate and preventing endonuclease accessibility. Consistent with this notion, at these same higher protein/DNA stoichiometries, H1 also inhibited the activity of DNase I and MNase (data not shown).

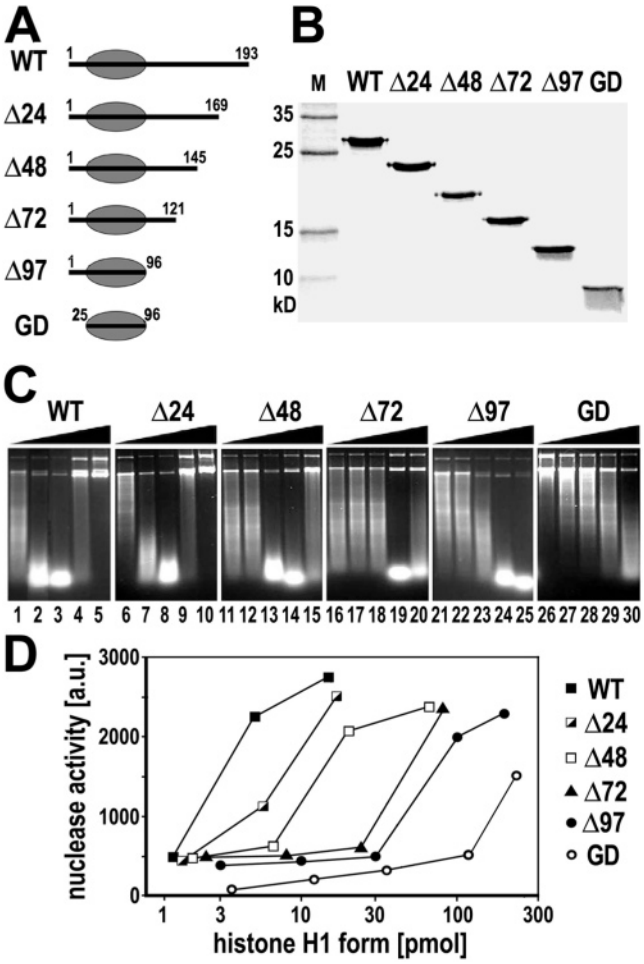

FIGURE 2: The histone H1 domain responsible for efficient stimulation of DFF40/CAD DNA cleavage is localized in the C-terminal region. (A) Diagram showing the structures of different bacterially expressed truncated forms of mouse histone H1-0. (B) SDS−PAGE of wild-type (WT) and truncated forms of histone H1-0. (C) Plasmid DNA cleavage by caspase-activated DFF in the presence of WT and truncated forms of histone H1 (30-, 100-, 300-, 1000-, and 2000-ng each). (D) Quantification of data shown in panel C. To quantitate data, electrophorograms were divided into zones where average DNA length was reduced 3-, 10-, and 30-fold, and the amount of DNA in each defined zone was obtained by density-scanning and multiplied by the reduction-in-length factor. Obtained values are presented in arbitrary units (a.u.; maximum value 3000). Amounts of histone H1 forms (*X*-axis) are expressed as picomoles in a log scale. Data for amounts of H1 forms where stimulatory effects were inhibited are not shown.

The C-Terminal Domain of Histone H1-0 Mediates Stimulation of DFF40/CAD Activity. To determine the segments within histone H1 that are responsible for DFF40/CAD stimulation, we initially examined the effects of a set of recombinant H1-0 truncation mutants (Figure 2A,B). These mutants previously have been used to define the H1 regions involved in stabilizing folded chromatin fibers (*6*). Activation of DFF40/CAD as a function of protein concentration was determined for each H1 CTD mutant (Figure 2C,D). At amounts between 1 and 15 pmol, H1-0 mutants lacking CTD residues 122−193 were incapable of activating the enzyme (Figure 2C,D, mutants Δ72, Δ97, and GD). These results demonstrate that, at physiologically relevant H1/DNA ratios, the H1 CTD is required for DFF40/CAD activation. Examination of the other CTD truncation mutants (Δ24, Δ48, and Δ72) showed that H1-0 mutants lacking the

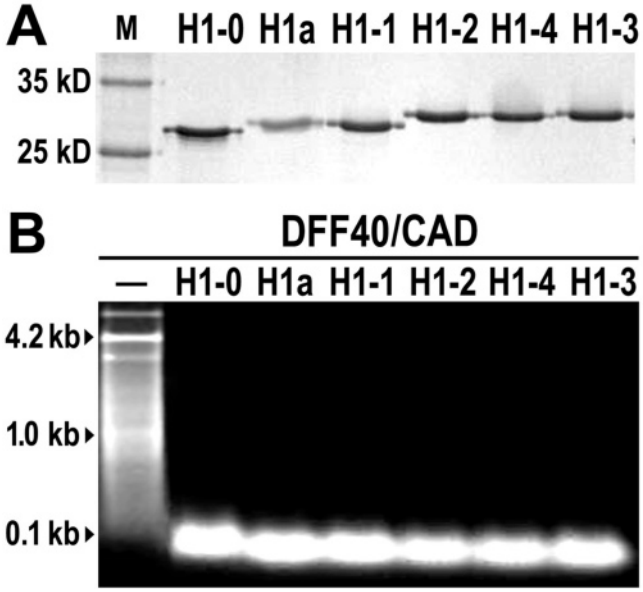

FIGURE 3: Different histone H1 subtypes similarly stimulate DNA cleavage by DFF40/CAD. (A) SDS−PAGE of purified mouse histone H1 subtypes (M, molecular mass standards). (B) Plasmid DNA cleavage by activated DFF40/CAD in the presence of different histone H1 subtypes (10 pmol each) and with reactions carried out at 100 mM NaCl.

C-terminal most 24, 48, and 72 amino acid residues required successively more protein to maximally stimulate DFF40/CAD activity compared to full-length H1-0 (Figure 2C,D). Thus, no single short segment or motif within CTD residues 122−193 appears to mediate H1-dependent DFF40/CAD activation. Interestingly, at high protein concentrations (>75 pmol), the NTD-GD segment of H1 (Δ97 mutant) was even capable of activating the nuclease, and deletion of residues 1−24 of the NTD resulted in a lessening of the GD to stimulate the activity of the nuclease (Figure 2C, compare lanes 24 and 29).

The data in Figure 2 also demonstrate that the inhibition of DFF40/CAD activity at higher protein concentrations was correlated with the extent of H1 CTD present (Figure 2C, compare lanes 4−5, 9−10, 14−15, 19−20, 24−25, 29−30). As increasing amounts of CTD were deleted, inhibition by the H1 fragments occurred at successively higher protein concentrations. In contrast, inhibition did not occur with the Δ97 mutant (residues 1−96) or H1-0 GD over this concentration range. These results are consistent with the effect being related to inhibitory H1−DNA interactions as described in the previous section. In fact, it has been shown that linker histone mutants with shorter CTDs have lower relative binding affinities to chromatin (*6*, *7*). Therefore, it is likely that linker histone mutants with shorter CTDs also have lower affinities to bind to naked DNA and, as a result, are required to have higher concentrations to inhibit DFF40/CAD activity.

Somatic Histone H1 Isotypes Equally Stimulate DFF40/CAD. The CTDs of the histone H1 isoforms differ significantly in primary sequence but not total amino acid composition (*6*). Thus, to determine the importance of CTD sequence in nuclease activation, we assayed whether the somatic H1 isotypes differentially stimulated DFF40/CAD. These experiments also addressed the hypothesis that H1-1, which has been demonstrated to trigger apoptosis in response

to DNA damage (*16*), might be a preferential stimulator of DFF40/CAD. As shown in Figure 3, each of the six mouse somatic cell histone H1 isotypes equally and robustly stimulate DFF40/CAD activity at low concentration (10 pmol). In addition, each of these six isotypes exhibited very similar activity response curves over a wide concentration range, and at high concentration (50 pmol), each H1 isotype equally inhibited DNA cleavage (data not shown). We also found similar results when we tested the human somatic cell histone H1 isoforms (data not shown). Thus, the ability of the H1 CTD to activate DFF40/CAD is unrelated to amino acid sequence. A more important determinant appears to be amino acid composition.

Histone H1-0 CTD Peptides Differentially Activate DFF40/CAD. In view of the results obtained in Figures 2 and 3, we next determined the ability of synthetic CTD fragments to activate DFF40/CAD. Peptides encompassing the following CTD residues were tested: 97−193 (full-length CTD), 97−169, 97−145, 121−145, 122−169, and 146−193 (Figure 4A,B). At 10 pmol peptide, fragments 97−169, 122−169, 146−193, and the intact CTD were able to potently activate DFF40/CAD (Figure 4C,D). Fragment 97−145 was significantly less effective at this concentration, consistent with the CTD truncation data. Importantly, although fragment 122−169 was able to activate the enzyme, fragment 121−145 was incapable of activating DFF40/CAD. Thus, the minimum CTD segment length required for nuclease activation appears to be greater than 24 residues. As was observed with the full-length H1 and H1 CTD truncation mutants (Figure 2), the specific CTD peptides that activated DFF40/CAD at low concentration also caused inhibition of DFF40/CAD at higher protein concentrations.

The Histone H1-0 CTD Binds to DFF Species. Previously, we have shown that wild-type histone H1 binds to DFF species using an immunoprecipitation assay with antibody against DFF45 (*14*). We have extended this observation by characterizing the binding of H1-0 and H1-0 CTD fragments to both DFF heterodimers and DFF40/CAD homo-oligomers using pore-exclusion limit electrophoresis and Western blotting (Figure 5). As shown in Figure 5A, DFF40/CAD homo-oligomers bind full-length histone H1-0 and the isolated H1-0 CTD but not the H1-0 Δ97 mutant lacking the CTD. In this assay, binding is evidenced by the disappearance of material from the gel. This is because the pH of the running buffer is 9.5 (very close to the 9.2 pI of DFF40) and the DFF species becomes positively charged upon binding highly basic histone H1 proteins. Importantly, we also found, using this assay, that three different CTD fragments (97−145, 122−169, and 146−193) each bind to DFF40/CAD homo-oligomers (the latter two being the most potent). Interestingly, wild-type H1 and the H1 CTD, but not the Δ97 mutant, also bind to DFF45/ICAD monomers (Figure 5B). We obtained the same result for actin but not for BSA (data not shown), indicating that the histone H1 CTD has the ability to specifically associate with other proteins besides DFF40/CAD.

Association of the Histone H1-0 CTD with DFF Species Converts Them into DNA Binding Proteins. To determine whether histone H1 association with DFF species enhances DNA binding, we utilized a DNA cellulose bead assay. Protein species bound to the beads were identified in eluates using Western blotting from SDS−PAGE gels. As shown

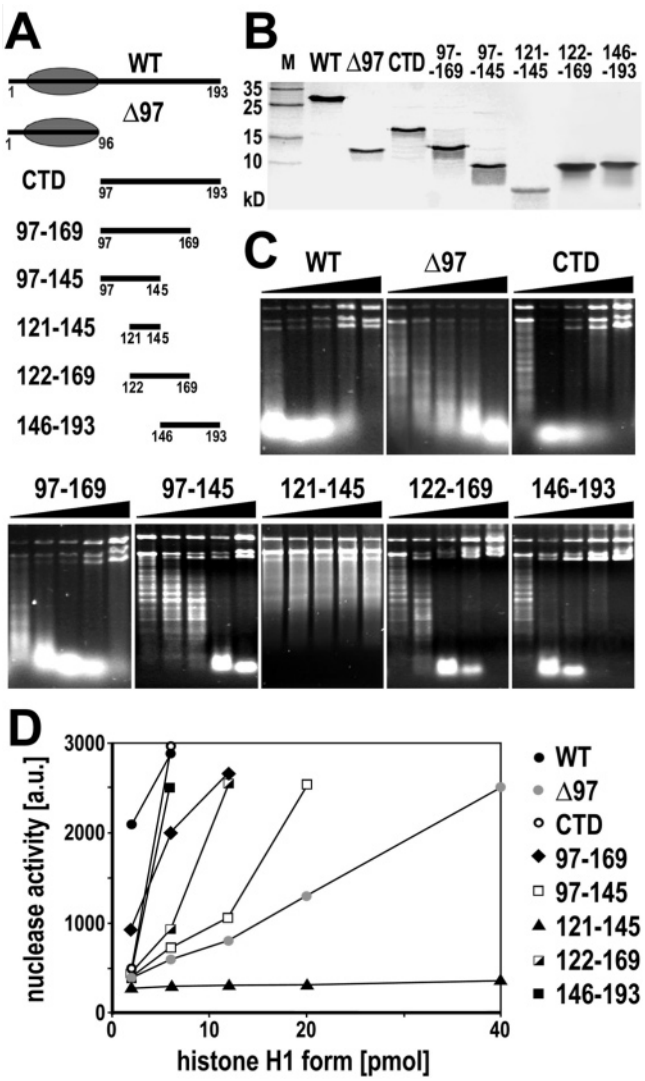

FIGURE 4: Mapping the C-terminal domain of histone H1 responsible for stimulation of DNA cleavage by caspase-activated DFF. (A) Diagram showing structure of different bacterially expressed or synthetic truncated forms of mouse histone H1-0. (B) SDS−PAGE of WT and truncated forms of histone H1-0. (C) Plasmid DNA was cleaved by DFF40/CAD in the presence of equimolar amounts (2-, 6-, 12-, 20-, and 40-pmol) of WT and truncated forms of histone H1-0. (D) Quantification of data shown in panel C. To quantitate data, electrophorograms were divided into zones where average DNA length was reduced 3-, 10-, and 30-fold, and the amount of DNA in each defined zone was obtained by density-scanning and multiplied by the reduction-in-length factor. Obtained values are presented in arbitrary units (a.u.; maximum value 3000). Amounts of histone H1 forms (*X*-axis) are expressed as picomoles in a log scale. Data for amounts of H1 forms where stimulatory effects were inhibited are not shown.

in Figure 6A, histone H1 was recovered from DNA cellulose whenever it was present in input protein mixtures. DFF heterodimers bound to the beads only when histone H1 was also present, and caspase-3-treated DFF40/CAD binding to DNA cellulose was increased several fold in the presence of histone H1 (Figure 6A). Figure 6B demonstrates that the CTD, but not the Δ97 mutant, conferred DNA binding ability to DFF40/CAD. In addition, we found that three CTD fragments (97−145, 122−169, and 146−193) also enhance binding of caspase-activated DFF40/CAD to DNA cellulose (yet fragment 97−145 was less effective in such enhancement, Figure 6B). In conclusion, we have demonstrated that

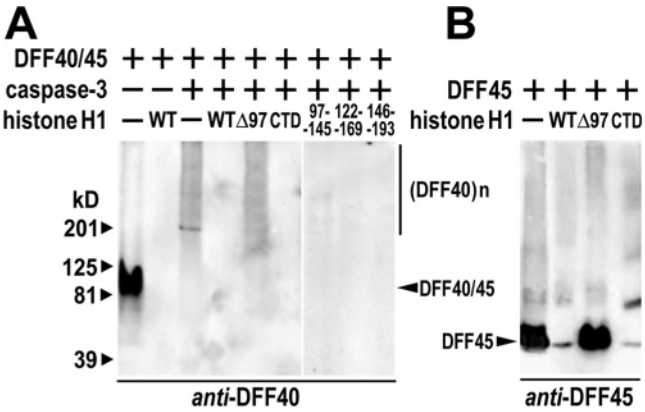

FIGURE 5: Histone H1 and its C-terminal domain bind to DFF. (A) DFF heterodimers (1 μg) or caspase-activated DFF were incubated with either the full-length (WT; 2 μg), its N-terminal/globular (Δ97; 1 μg) or C-terminal (CTD; 1 μg) domains of histone H1-0, or peptides 97−145, 122−169, and 146−193 (1 μg). Protein complexes were resolved by 4−24% polyacrylamide gradient pore-exclusion limit electrophoresis and detected by Western blotting using anti-DFF40 antibodies. The same analysis was done for purified DFF45 (panel B).

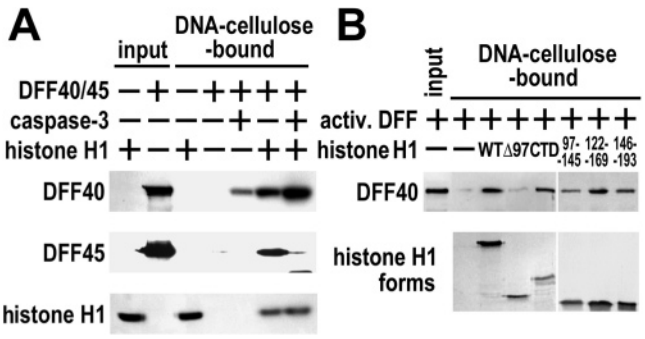

FIGURE 6: Histone H1 and its C-terminal domain enhance the DNA binding of DFF heterodimers and caspase-activated DFF. (A) DFF heterodimers or caspase-activated DFF were incubated with total HeLa cell histone H1 and then with DNA−cellulose. Cellulose beads were washed and bound proteins eluted with SDS. Eluted proteins were separated by SDS−PAGE and detected by Western blotting using the indicated antibodies. (B) Caspase-activated DFF was incubated with either full-length (WT), N-terminal/globular (Δ97), or C-terminal (CTD) domains of histone H1-0 or peptides 97−145, 122−169, and 146−193, and its binding to DNA−cellulose was analyzed as in panel A.

the CTD of histone H1-0 and several CTD fragments bind to DFF and stimulate both its enzymatic activity and DNA binding.

DISCUSSION

DFF40/CAD is known to exhibit an extraordinary preference for cleaving the internucleosomal linker regions in chromatin (*15*). This preference stems from the scissors-like structure of the DFF40/CAD active site (*28*). We propose this preference for linker DNA is significantly enhanced by binding of histone H1 to the enzyme. Indeed, histone H1 is known to be in rapid equilibrium with its nucleosomal binding sites in living cells and is not statically bound to nucleosomes (*7*, *30*−*32*). Thus, it is readily available for binding to other nuclear proteins. Over 15 different proteins have been shown to bind to histone H1 mostly by in vitro experiments (*33*−*44*), including the DFF45 monomers, DFF heterodimers, and DFF40/CAD homo-oligomers characterized in our study. Clearly, the mechanisms through which histone H1 mediates nuclear functions must involve protein−protein interactions in addition to its well-documented effect on chromatin architecture.

We found that each of the six somatic cell histone H1 isoforms equally activated DFF40/CAD in vitro. The same results have been obtained for H1-dependent stabilization of folded chromatin (X.L., M.H.P, J.C.H, unpublished). Because histone H1 isoforms are expressed at different levels in various cell types, this lack of specificity will allow apoptotic DNA degradation or chromatin condensation to occur in all cells independent of differences in isoform ratios. The amino acid sequence of the CTD varies considerably between H1 isoforms, and yet, the amino acid composition of the CTDs is remarkably similar (ref *6*; see below). The importance of amino acid composition rather than sequence may be related to the role of intrinsic disorder in CTD function (see below). Thus, it may not be particularly surprising that each isoform can strongly activate DFF40/CAD. Also, it is not uncharacteristic for several H1 isoforms to display an activity in vitro, but that only one will display in vivo (*45*).

In the case of DFF40/CAD function, we envision several roles for H1 interactions relating to potentiation of genome fragmentation during apoptosis. In our working model, H1 binding first helps overcome the cleavage barrier posed by condensed chromatin by activating DFF40/CAD. The experimental evidence for this comes from previous studies showing that condensed, in vitro-reconstituted nucleosomal templates containing histone H1 were much more effectively cleaved by DFF40/CAD in comparison with MNase (*14*). Given the evidence that condensed chromatin, in vivo, contains a more heterogeneous mix of all somatic subtypes compared to euchromatin (*46*, *47*), the lack of specificity of DFF40 for any one subtype in vitro could suggest a reason condensed nucleosomal templates can be effectively cleaved by DFF40/CAD in vivo. As the cleaved chromatin fragments become successively shorter than six nucleosomes long, the chromatin fragments will progressively decondense (*2*), and H1 will be free to maximally stimulate the nuclease to complete genome fragmentation. We also envision that the transient free pool of nucleoplasmic H1 present due to rapid equilibrium exchange of H1 from its chromatin binding sites (*7*, *30*−*32*) could allow free DFF40/CAD to associate with the H1 and be recruited to histone H1-free-chromatin fragments through the H1 GD, which is also known to mediate nucleosomal DNA binding (*5*). Hence, it is easy to model several ways in which H1 binding may potentiate chromatin linker DNA cleavage by DFF40/CAD.

The data in Figures 2−6, to the best of our knowledge, are the first to demonstrate the histone H1 CTD is able to specifically mediate protein−protein interactions. From a protein chemistry perspective, the H1 CTD is enigmatic. While long considered to be an unstructured polycation that binds DNA during chromatin condensation (*2*, *3*), this mechanism has recently been ruled out in vitro (*6*) and in vivo (*7*). Instead, the CTD appears to stabilize folded chromatin through a mechanism involving "intrinsic disorder" (*6*, *48*, *49*, and references therein). Intrinsically disordered regions of proteins often appear to be combinatorial interaction domains that are unstructured in the absence of macromolecular interactions and assume secondary structures when bound to different macromolecular partners (*48*, *49*).

Our observation that the H1 CTD can mediate specific protein−protein interactions with DFF40/CAD, together with the previous findings that the H1 CTD alters linker DNA structure and stabilizes condensed secondary and tertiary chromatin structures when bound to chromatin fibers (*6*), demonstrates that the histone H1 CTD is able to participate in multiple interactions with different macromolecular partners. Furthermore, when H1 is bound to DNA in vitro, a segment of the CTD is induced to form an amphipathic helix (*50*, *51*). In many ways, the H1 CTD is reminiscent of acidic activation domains such as VP16, which are capable of interacting with many different transcription factors and coactivators, for example, TBP, TFIIA, and P300 (*52*, *53*). VP16 alone is unstructured, but assumes an α-helical structure as a consequence of interaction with proteins such as PC4 (*53*). Modulation of macromolecular interactions through coupled secondary chromatin structure formation is an emerging theme in structural biology (*48*, *49*).

We have previously shown that the regions of the H1-0 CTD that stabilize condensed chromatin fibers are located in two distinct subdomains encompassing residues 97−121 and 146−169 (*6*). In contrast, the region responsible for DFF40/CAD activation appears to be spread throughout residues 122−193 (Figures 2 and 4). Interestingly, all CTD peptides ≥47 residues in length were able to effectively activate DFF40/CAD, regardless of their location in the intact CTD (Figure 4), and each of these peptides have very similar amino acid compositions. One vision of H1 stucture in vivo has the region encompassed by residues 146−169 on the CTD responsible for bending linker DNA, while the entire CTD is actually positioned such that it limits the accessibility of proteins to the GD in an intact chromatosome structure (*54*). Hence, CTD sequences more distal to the GD would be more easily accessible to other proteins such as DFF40. This could explain why, of the three 48 residue fragments investigated in Figure 4, residues 146−193 and 122−169 show somewhat greater activity than fragment 97−145. Such a fragment proximal to the GD may not have the same evolutionary pressures for interacting with apoptotic nucleases, hence, evolving into a less optimal region for DFF40 binding, as evidenced with the result in Figure 6B. Thus, in addition to amino acid composition, length and location within the H1 CTD may also be important interaction determinants.

ACKNOWLEDGMENT

We thank Dr. Gregor Meiss (JLU Giessen, Germany) for a CAD-GST expression vector. Peptide synthesis and mass spectrometry services were kindly provided by the Protein Chemistry Technology Center at UT Southwestern Medical Center.

REFERENCES

1. Luger, K., Mäder, A. W., Richmond, R. K., Sargent, D. F., and Richmond, T. J. (1997) Crystal structure of the nucleosome core particle at 2.8 Angstrom resolution, *Nature 389*, 251−260.
2. Van Holde, K. E. (1988) *Chromatin*, Springer-Verlag, New York.
3. Ramakrishnan, V. (1997) Histone H1 and chromatin higher-order structure, *Crit. Rev. Eukaryotic Gene Expression 7*, 215−230.
4. Khochbin, S. (2001) Histone H1 diversity: bridging regulatory signals to linker histone function, *Gene 271*, 1−12.
5. Vignali, M., and Workman, J. L. (1998) Location and function of linker histones, *Nat. Struct. Biol. 5*, 1025−1028.
6. Lu, X., and Hansen, J. C. (2004) Identification of specific functional subdomains within the linker histone $H1^0$ C-terminal domain, *J. Biol. Chem. 279*, 8701−8707.
7. Hendzel, M. J., Lever, M. A., Crawford, E., and Th'ng, J. P. H. (2004) The C-terminal domain is the primary determinant of histone H1 binding to chromatin in vivo, *J. Biol. Chem. 279*, 20028−20034.
8. Fan, Y., Nikitina, T., Morin-Kensicki, E. M., Zhao, J., Magnuson, T. R., Woodcock, C. L., and Skoultchi, A. I. (2003) H1 linker histones are essential for mouse development and affect nucleosome spacing in vivo, *Mol. Cell. Biol. 23*, 4559−4572.
9. Zhang, J., and Xu, M. (2002) Apoptotic DNA fragmentation and tissue homeostasis, *Trends Cell Biol. 12*, 84−89.
10. Yasutomo, K., Horiuchi, T., Kagami, S., Tsukamoto, H., Hashimura, C., Urushihara, M., and Kuroda, Y. (2001) Mutation of DNASE1 in people with systemic lupus erythematosus, *Nat. Genet. 28*, 313−314.
11. Nupirei, M., Karsunky, H., Zevnik, B., Stephan, H., Mannherz, H. G., and Möröy, T. (2000) Features of systemic lupus erythematosus in DNase-1 deficient mice, *Nat. Genet. 25*, 177−181.
12. Widlak, P., and Garrard, W. T. (2005) Discovery, regulation and action of the major apoptotic nucleases DFF40/CAD and endonuclease G, *J. Cell. Biochem. 94*, 1078−1087.
13. Liu, X., Li, P., Widlak, P., Zou, H., Luo, X., Garrard, W. T., and Wang, X. (1998) The 40-kDa subunit of DNA fragmentation factor induces DNA fragmentation and chromatin condensation during apoptosis. *Proc. Natl. Acad. Sci. U.S.A. 95*, 8461−8466.
14. Liu, X., Zou, H., Widlak, P., Garrard, W., and Wang, X. (1999) Activation of the apoptotic endonuclease DFF40 (caspase-activated DNase or nuclease): oligomerization and direct interaction with histone H1, *J. Biol. Chem. 274*, 13836−13840.
15. Widlak, P., Li, P., Wang, X., and Garrard, W. T. (2000) Cleavage preferences of the apoptotic nuclease DFF40 (caspase-activated DNase or nuclease) on naked DNA and chromatin substrates, *J. Biol. Chem. 275*, 8226−8232.
16. Konishi, A., Shimizu, S., Hirota, J., Toshifumi, T., Fan, Y., Matsuoka, Y., Zhang, L., Yoneda, Y., Fujii, Y., Skoultchi, A. I., and Tsujimoto, Y. (2003) Involvement of histone H1.2 in apoptosis induced by DNA double-strand breaks, *Cell 114*, 673−688.
17. Parseghian, M. H., Henschen, A. H., Krieglstein, K. G., and Hamkalo, B. A. (1994) A proposal for a coherent mammalian histone H1 nomenclature correlated with amino acid sequences, *Protein Sci. 3*, 575−587.
18. Korn, C., Scholz, S. R., Gimadutdinow, O., Pingoud, A., and Meiss, G. (2002) Involvement of conserved histidine, lysine and tyrosine residues in the mechanisms of DNA cleavage by the caspase-3 activated DNase CAD, *Nucleic Acids Res. 30*, 1325−1332.
19. Widlak, P., Gaynor, R. B., and Garrard, W. T. (1997) In vitro chromatin assembly of the HIV-1 promoter, *J. Biol. Chem. 272*, 17654−17661.
20. Parseghian, M. H., Clark, R. F., Hauser, L. J., Dvorkin, N., Harris, D. A., and Hamkalo, B. A. (1993) Fractionation of human H1 subtypes and characterization of a subtype-specific antibody exhibiting non-uniform nuclear staining, *Chromosome Res. 1*, 127−139.
21. Mizzen, C. A., Alpert, A. J., Levesque, L., Kruck, T. P. A., and McLachlan, D. R. (2000) Resolution of allelic and non-allelic variants of histone H1 by cation-exchange-hydrophilic-interaction chromatography, *J. Chromatogr., B 744*, 33−46.
22. Sambrook, J., Fritsch, E. F., and Maniatis, T. (1989) Molecular cloning: a laboratory manual, 2nd ed, Vol. 3, Cold Spring Harbor Laboratory, Cold Spring Harbor, NY.
23. Fields, C. G., Lloyd, D. H., MacDonald, R. L., Otteson, K. M., and Noble, R. L. (1991) HBTU activation for automated Fmoc solid-phase peptide synthesis, *Peptide Res. 4*, 95−101.
24. Widlak, P., Lanuszewska, J., Cary, R. B., and Garrard, W. T. (2003) Subunit structures and stoichiometries of human DFF proteins before and after induction of apoptosis, *J. Biol. Chem. 278*, 26915−26922.
25. Enari, M., Sakahira, H., Yokoyama, H., Okawa, K., Iwamatsu, A., and Nagata, S. (1998) A caspase-activated DNase that degrades DNA during apoptosis, and its inhibitor ICAD, *Nature 391*, 43−50.
26. Sakahira, H., Enari, M., and Nagata, S. (1998) Cleavage of CAD inhibitor in CAD activation and DNA degradation during apoptosis, *Nature 391*, 96−99.

27. Halenbeck, R., MacDonald, H., Roulston, A., Chen, T. T., Conroy, L., and Williams, L. T. (1998) CPAN, a human nuclease regulated by the caspase-sensitive inhibitor DFF45, *Curr. Biol. 8*, 537−540.
28. Woo, E.-J., Kim, Y.-G., Kim, M.-S., Han, W.-D., Shin, S., Robinson, H., Park, S.-Y., and Oh, B.-H. (2004) Structural mechanism for inactivation and activation of CAD/DFF40 in the apoptotic pathway, *Mol. Cell 14*, 531−539.
29. Hud, N., Milanovich, F., and Balhorn, R. (1994) Evidence of novel secondary structure in DNA-bound protamine is revealed by Raman spectroscopy, *Biochemistry 33*, 7528−7535.
30. Lever, M. A., Th'ng, J. P., Sun, X., and Hendzel, M. J. (2000) Rapid exchange of histone H1.1 on chromatin in living human cells, *Nature 408*, 873−876.
31. Misteli, T., Gunjan, A., Hock, R., Bustin, M., and Brown, D. T. (2000) Dynamic binding of histone H1 to chromatin in living cells, *Nature 408*, 877−881.
32. Contreras, A., Hale, T. K., Stenoien, D. L., Rosen, J. M., Mancini, M. A., and Herrera, R. E. (2003) The dynamic mobility of histone H1 is regulated by cyclin/CDK phosphorylation, *Mol. Cell. Biol. 23*, 8626−8636.
33. Rasmussen, C., and Garen, C. (1993) Activation of calmodulin-dependent enzymes can be selectively inhibited by histone H1, *J. Biol. Chem. 268*, 23788−23791.
34. Swindle, C. S., and Engler, J. A. (1998) Association of the human papillomavirus type 11 E1 protein with histone H1, *J. Virol. 72*, 1994−2001.
35. Giampuzzi, M., Oleggini, R., and Di Donato, A. (2003) Demonstration of in vitro interaction between tumor suppressor lysyl oxidase and histones H1 and H2: definition of the regions involved, *Biochim. Biophys. Acta 1647*, 245−251.
36. Nielsen, A. L., Oulad-Abdelghani, M., Ortiz, J. A., Remboutsika, E., Chambon, P., and Losson, R. (2001) Heterochromatin formation in mammalian cells: interaction between histones and HP1 proteins, *Mol. Cell 7*, 729−739.
37. Ner, S. S., Blank, T., Perez-Paralle, M. L., Grigliatti, T. A., Becker, P. B., and Travers, A. A. (2001) HMG-D and histone H1 interplay during chromatin assembly and early embryogenesis, *J. Biol. Chem. 276*, 37569−37576.
38. Zhao, M., Sutherland, C., Wilson, D. P., Deng, J., Macdonald, J. A., and Walsh, M. P. (2004) Identification of the linker histone H1 as a protein kinase Cepsilon-binding protein in vascular smooth muscle, *Biochem. Cell. Biol. 82*, 538−546.
39. Erard, M. S., Belenguer, P., Caizergues-Ferrer, M., Pantaloni, A., and Amalric, F. (1988) A major nucleolar protein, nucleolin, induces chromatin decondensation by binding to histone H1, *Eur. J. Biochem. 175*, 525−530.
40. Lee, H., Habas, R., and Abate-Shen, C. (2004) Msx1 cooperates with histone H1b for inhibition of transcription and myogenesis, *Science 304*, 1675−1678.
41. Boulikas, T., Wiseman, J. M., and Garrard, W. T. (1980) Points of contact between histone H1 and the histone octamer, *Proc. Natl. Acad. Sci. U.S.A. 77*, 127−131.
42. Karetsou, Z., Sandaltzopoulos, R., Frangou-Lazaridis, M., Lai, C. Y., Tsolas, O., Becker, P. B., and Papamarcaki, T. (1998) Prothymosin a modulates the interaction of histone H1 with chromatin, *Nucleic Acids Res. 26*, 3111−3118.
43. Kondili, K., Tsolas, O., and Papamarcaki, T. (1996) Selective interaction between parathymosin and histone H1, *Eur. J. Biochem. 242*, 67−74.
44. Kohlstaedt, L. A., and Cole, R. D. (1994) Specific interaction between H1 histone and high mobility protein HMG1, *Biochemistry 33*, 570−575.
45. Ajiro, K., Shibata, K., and Nishikawa, Y. (1990) Subtype-specific cyclic AMP-dependent histone H1 phosphorylation at the differentiation of mouse neuroblastoma cells, *J. Biol. Chem. 265*, 6494−6500.
46. Parseghian, M. H., Newcomb, R. L., Winokur, S. T., and Hamkalo, B. A. (2000) The distribution of somatic H1 subtypes is non-random on active vs. inactive chromatin: distribution in human fetal fibroblasts, *Chromosome Res. 8*, 405−424.
47. Parseghian, M. H., Newcomb, R. L., and Hamkalo, B. A. (2001) The distribution of somatic H1 subtypes is non-random on active vs. inactive chromatin II: distribution in human adult fibroblasts, *J. Cell. Biochem. 83*, 643−659.
48. Dunker, A. K., Brown, C. J., Lawson, J. D., Iakoucheva, L. M., and Obradovic, Z. (2002) Intrinsic disorder and protein function, *Biochemistry 41*, 6573−6582.
49. Wright, P. E., and Dyson, H. J. (1999) Intrinsically unstructured proteins: re-assessing the protein structure−function paradigm, *J. Mol. Biol. 293*, 321−331.
50. Vila, R., Ponte, I., Collado, M., Arrondo, J. L., and Suau, P. (2001) Induction of secondary structure in a COOH-terminal peptide of histone H1 by interaction with DNA, *J. Biol. Chem. 276*, 30898−30903.
51. Vila, R., Ponte, I., Jimenez, M. A., Rico, M., and Suau, P. (2000) A helix-turn motif in the C-terminal domain of histone H1, *Protein Sci. 9*, 627−636.
52. Ptashne, M., and Gann, A. (1997) Transcriptional activation by recruitment, *Nature 386*, 569−577.
53. Jonker, H. R., Wechselberger, R. W., Boelens, R., Folkers, G. E., and Kaptein, R. (2005) Structural properties of the promiscuous VP16 activation domain, *Biochemistry 44*, 827−839.
54. Bharath, M. M. S., Chandra, N. R., and Rao, M. R. S. (2003) Molecular modeling of the chromatosome particle, *Nucleic Acids Res. 31*, 4264−4274.

BI050100N